



Supplementary Information for

Heterogeneous iodine-organic chemistry fast-tracks marine new particle formation

Ru-Jin Huang^{a,b,c,d,1}, Thorsten Hoffmann^e, Jurgita Ovadnevaite^f, Ari Laaksonen^{g,h}, Harri Kokkola^g, Wen Xu^{i,j}, Wei Xu^{a,f}, Darius Ceburnis^f, Renyi Zhang^{i,j}, John H. Seinfeld^{k,l}, Colin O'Dowd^f

^aState Key Laboratory of Loess and Quaternary Geology, Center for Excellence in Quaternary Science and Global Change, Institute of Earth Environment, Chinese Academy of Sciences, Xi'an 710061, China

^bOpen Studio for Oceanic-Continental Climate and Environment Changes, Pilot National Laboratory for Marine Science and Technology (Qingdao), Qingdao 266000, China

^cInstitute of Global Environmental Change, Xi'an Jiaotong University, Xi'an 710049, China

^dUniversity of Chinese Academy of Sciences, Beijing 100039, China

^eDepartment of Chemistry, Johannes Gutenberg University of Mainz, 55128 Mainz, Germany

^fSchool of Physics, Ryan Institute's Centre for Climate and Air Pollution Studies, National University of Ireland Galway, Galway H91 CF50, Ireland

^gFinnish Meteorological Institute, 00560 Helsinki, Finland

^hDepartment of Applied Physics, University of Eastern Finland, 70210 Kuopio, Finland

ⁱDepartment of Atmospheric Sciences, Texas A&M University, College Station, TX 77843

^jDepartment of Chemistry, Texas A&M University, College Station, TX 77843

^kDivision of Chemistry and Chemical Engineering, California Institute of Technology, Pasadena, CA 91125

^lDivision of Engineering and Applied Science, California Institute of Technology, Pasadena, CA 91125

¹To whom correspondence may be addressed. Email: rujin.huang@ieecas.cn

This PDF file includes:

Text for marine air observation
Figures S1 to S10

Marine air observation

The ambient measurements are continuously undertaken at the Mace Head Global Atmosphere Watch Research Station, located on the west coast of Ireland. These open ocean new particle formation events are detected quite frequently. Over a period of 10 years (2008-2018), we observed over 80 events with steady growth lasting longer than 6 hours under clean marine conditions. These events occurred in marine air masses with 57% of occurrence in maritime Polar (*mP*), 36% of maritime Arctic (*mA*), and 17% of maritime Tropical (*mT*) air masses. Our previous statistical analysis shown that the product of such events (namely open ocean nucleation and growth particles) was observed for 33% of the whole year (1), indicating such events are regular and important sources of particle in the marine atmosphere. Fig. S1 shows the geographical distribution of air mass backward trajectory frequency, indicating that such event is not related to specific or special meteorological conditions in the marine (Polar) air masses.

Figure S2 shows the 72-hour air mass backward trajectories during a typical open ocean event observed in June 2012 at Mace Head. The impact of coastal nucleation was considered to be minor during this event, because: 1) coastal nucleation typically occurs rapidly over much shorter timescales and is readily detected with much higher particle number concentration (up to and above 10^5 cm^{-3}) of sub 10 nm particles; 2) the uniform growth rate of this event was modest at 1 nm hour^{-1} , which was similar to the growth event observed during the Northeast Atlantic ocean cruise (2); 3) coastal nucleation is typically observed during low tide, however, this event had no tidal pattern; 4) the continuous particle growth over many hours is usually attributed to regional-scale particle formation, which is the open ocean in this case. In summary, the coastal events are readily distinguishable from the open ocean ones.

Figure S3 shows the boundary layer structure during sequential open ocean new particle formation events. It shows a decoupled boundary layer with buffered interaction with the free troposphere. The boundary layer in *mP* air masses is typically meteorologically-unstable, leading to vertical mixing typically limited to the boundary layer, but is rather well mixed and capped by a residual layer, resulting in pseudo-stationary periods where particle production and growth can be sustained for many hours.

References

1. M. Dall'Osto, A statistical analysis of North East Atlantic (submicron) aerosol size distributions. *Atmos. Chem. Phys.*, **11**, 12567-12578 (2011).
2. M. Ehn *et al.*, Growth rates during coastal and marine new particle formation in western Ireland. *J. Geophys. Res. Atmos.* **115**, <https://doi.org/10.1029/2010jd014292> (2010).
3. C. O'Dowd, C. Monahan, M. Dall'Osto, On the occurrence of open ocean particle production and growth events. *Geophys. Res. Lett.* **37**, L19805 (2010).

4. G. Martucci, C. D. O'Dowd, Ground-based retrieval of continental and marine warm cloud microphysics. *Atmos. Meas. Tech.* **4**, 2749-2765 (2011).

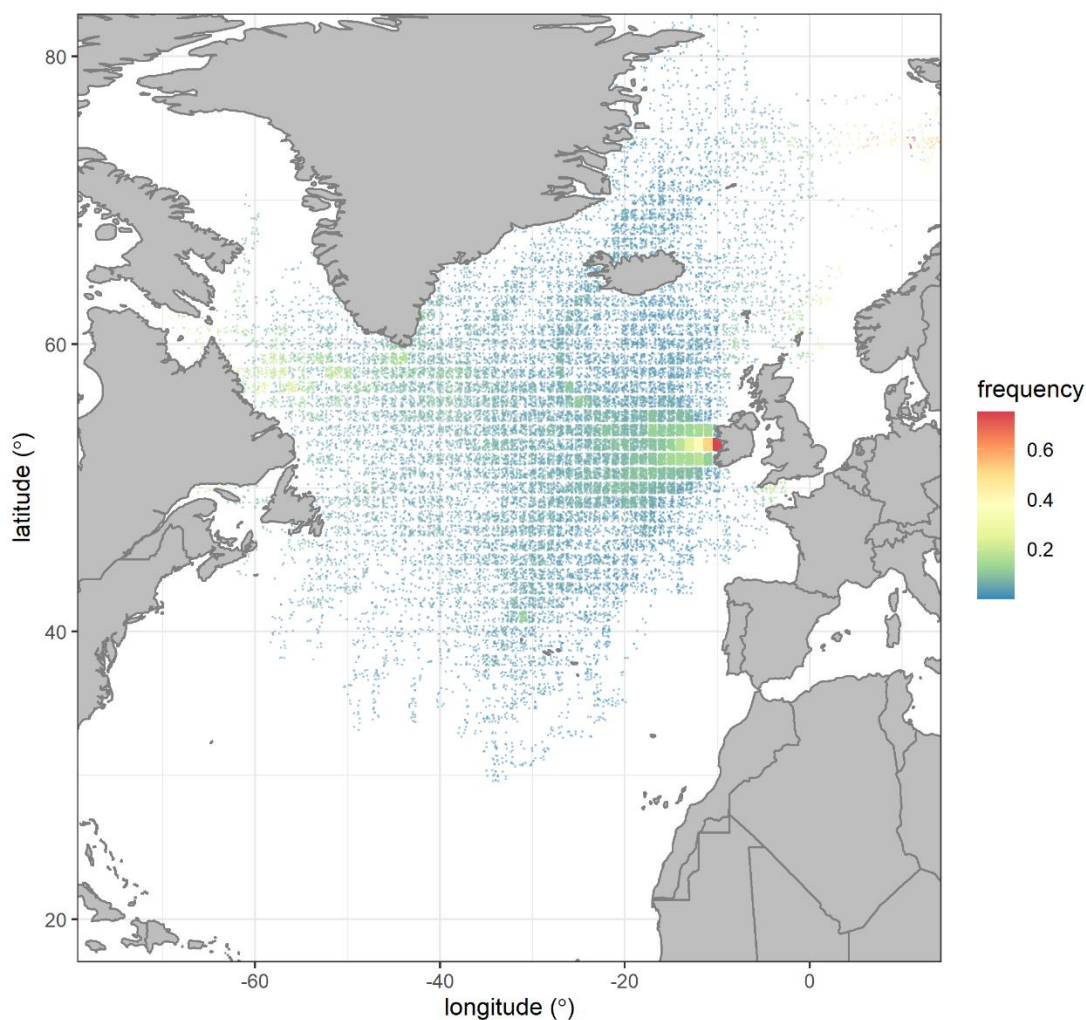


Fig. S1. The geographical distribution of the longitude-normalized frequency of 3-days air mass backward trajectories during the aerosol growth events observed at Mace Head station from 2008 to 2018. The color code at each pixel indicates the frequency of occurrence. The air masses were tracked using Hybrid Single-Particle Lagrangian Integrated Trajectory (HYSPLIT1) according to the Global Data Assimilation System (<https://www.ncdc.noaa.gov/data-access/model-data/model-datasets/global-data-assimilation-system-gdas>).

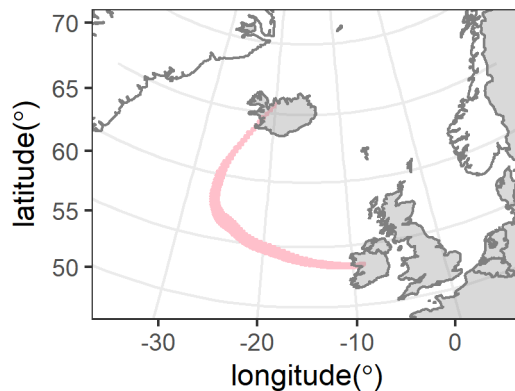


Fig. S2. Retrieved 72-hour air mass backward trajectories during the event. No precipitation was observed during this event; the air temperature ranged between 9.6 to 13.0 °C and the averaged wind speed was 3.8 m s⁻¹. The growth rate was 0.8 nm hour⁻¹, assuming that the growth rate during the nucleation stage was maintained throughout the event. The geographical location of the nucleation event is between Iceland and Ireland, indicating its marine origin. This event is a typical open ocean event, reported by a statistical study of (3) and regularly observed at Mace Head station and over the North Atlantic (2).

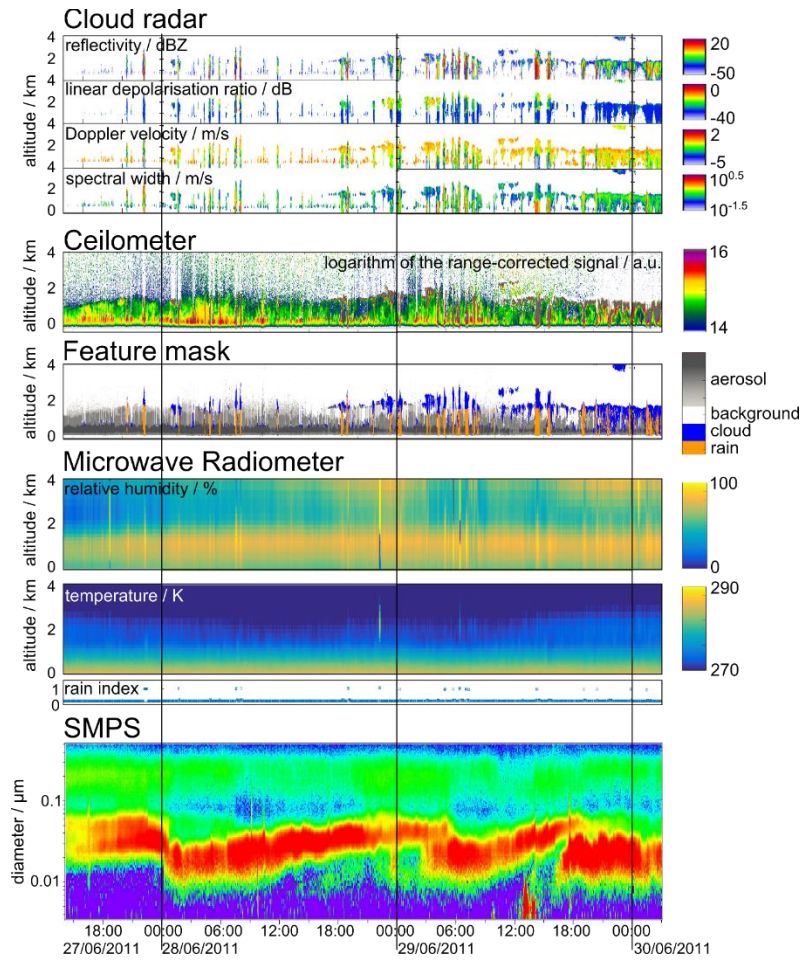


Fig. S3. A composite plot of boundary layer structure during sequential open ocean new particle formation events showing a continuously well mixed boundary layer with the residual layer above interspersed with precipitating small cumulus. Note that the plot is characterizing new particle formation events similar to those presented in the main text, due to instrumental data gaps. The boundary layer structure is revealed by the ground-based remote sensing system consisting of cloud radar, microwave radiometer and ceilometer described in detail by Martucci and O’Dowd (4).

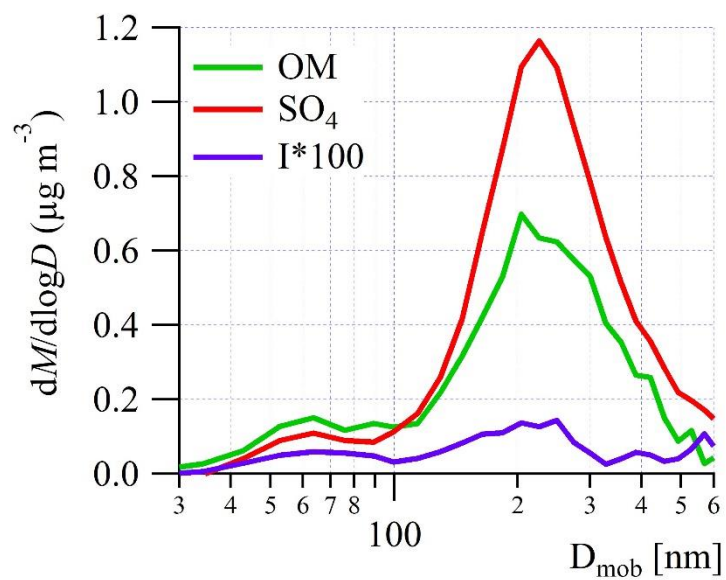


Fig. S4. The mass distributions of organic matter (OM), sulphate and iodine as retrieved from HR-ToF-AMS and averaged for the total event period. Iodine signal at m/z 127 is multiplied by 100. To be consistent with the SMPS measurements, AMS-derived vacuum aerodynamic diameter was converted to mobility diameter.

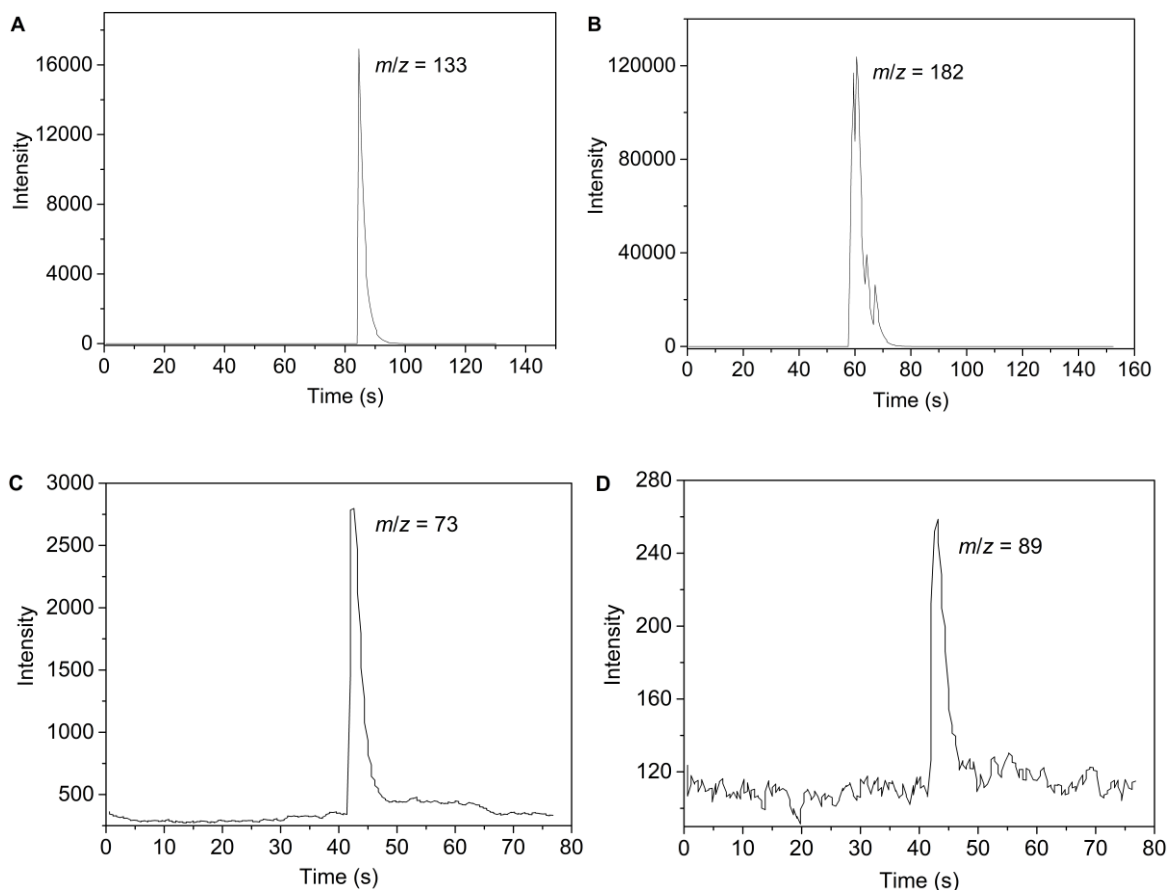


Fig. S5. Chemical characterization of the low-volatility organic acids formed from the heterogeneous reactions on nanoparticles using a thermal desorption-ion drift chemical ionization mass spectrometer (TD-ID-CIMS). (A) mass at $m/z = 133$ for IOP particles exposed to meso-erythritol is assigned as a protonated tartaric acid with a loss of H_2O , $[\text{C}_4\text{H}_6\text{O}_6 + \text{H} - \text{H}_2\text{O}]^+$, measured in positive MS mode. (B) The product of tartaric acid from meso-erythritol exposure is further confirmed by mass at $m/z = 182$, assigned as a negatively charged tartaric acid, measured in negative MS mode. (C) masses at $m/z = 73$ and (D) $m/z = 89$ for IOP particles exposed to glyoxal, assigned as a deprotonated glyoxylic acid $[\text{C}_2\text{H}_2\text{O}_3 - \text{H}]^-$ and oxalic acid $[\text{C}_2\text{H}_2\text{O}_4 - \text{H}]^-$, respectively. The sample was heated to $300\text{ }^\circ\text{C}$ to completely evaporate the collected mass when heating was applied at about 42 s (A, C, and D) and 58 s (B). The reagent ions were H_3O^+ and $\text{CO}_3^-/\text{CO}_4^-$ for A and B-D, respectively.

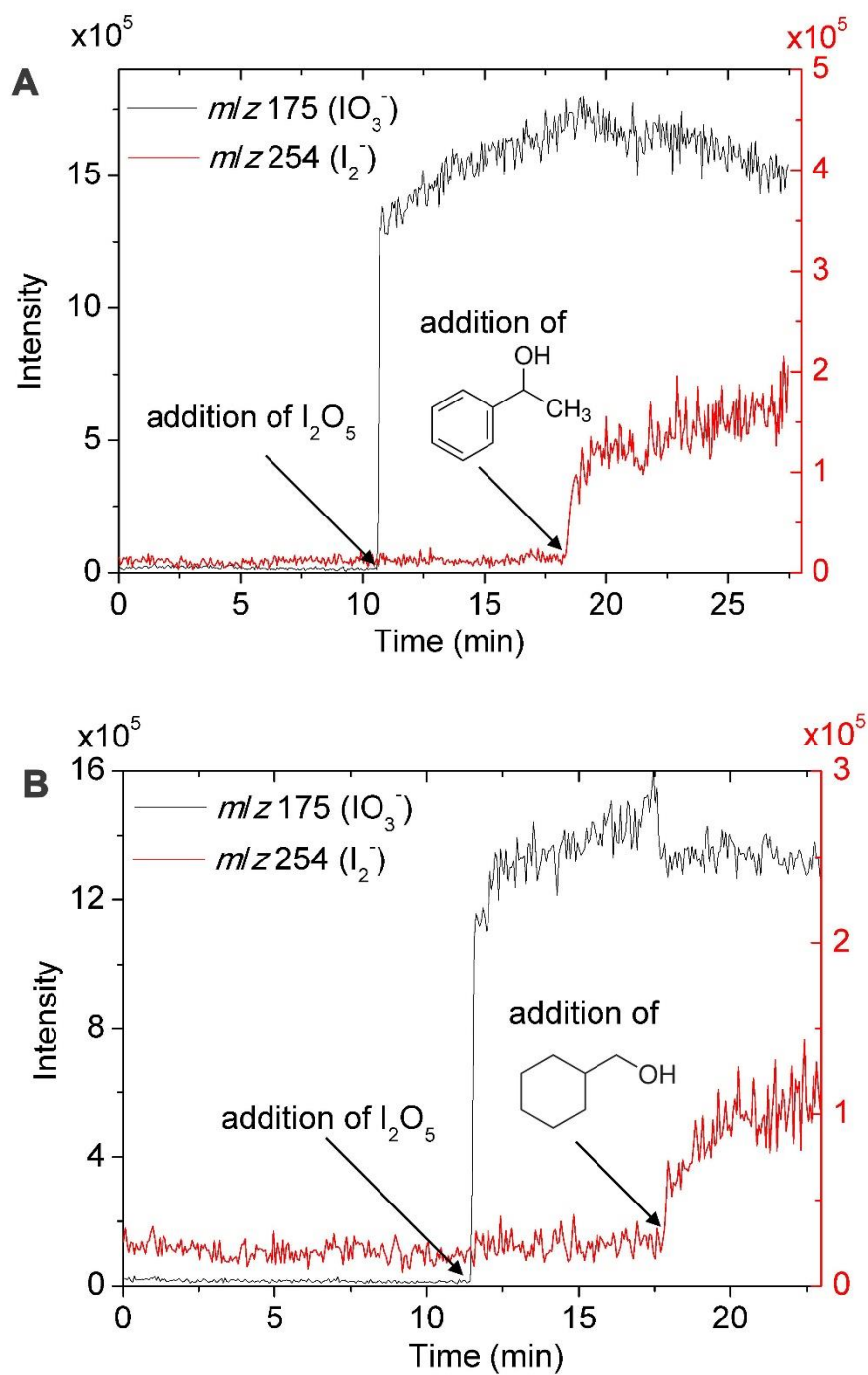


Fig. S6. Online APCI-MS analysis of products formed from I_2O_5 reduction by (A) 1-phenylethanol and (B) cyclohexanemethanol in particle phase. I_2O_5 hydrolyzed in aerosol water leading to the production of IO_3^- , which can be seen from the m/z 175 signal. IO_3^- was rapidly reduced to form I_2 as soon as 1-phenylethanol or cyclohexanemethanol was introduced into the reaction system, inferred from a rapid decrease of IO_3^- signal and increase of I_2^- (m/z 254) signal.

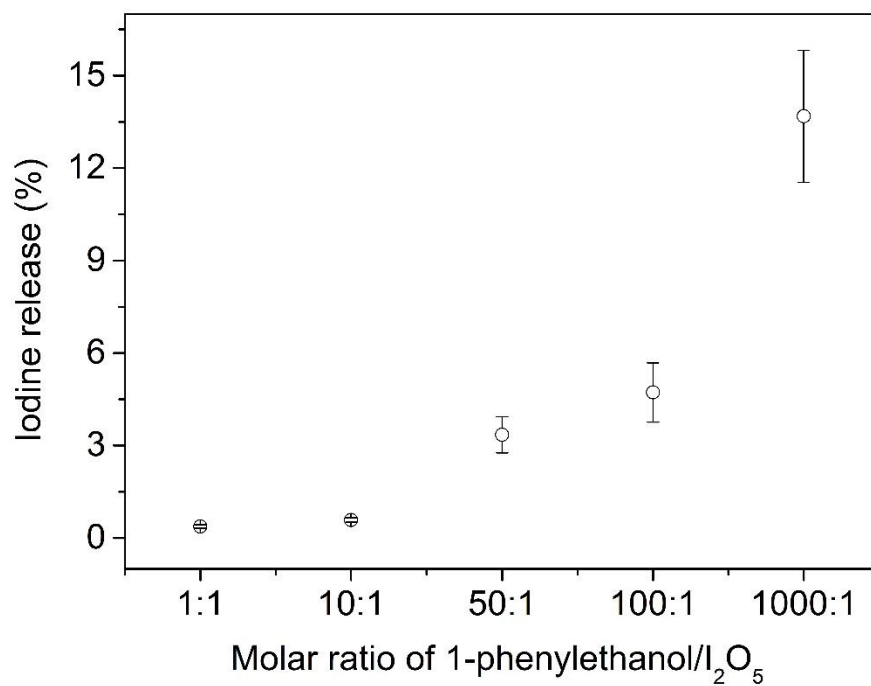


Fig. S7. Quantification of the released I₂ formed from IO₃⁻ (product of I₂O₅ hydrolysis) reduction by 1-phenylethanol in the particle phase, as a function of molar ratio of reactants. The pH of bulk solution is ~3. Errors (2σ) ranged between 5.2% and 20.4% and were determined from triplicate runs of three individual experiments for each data.

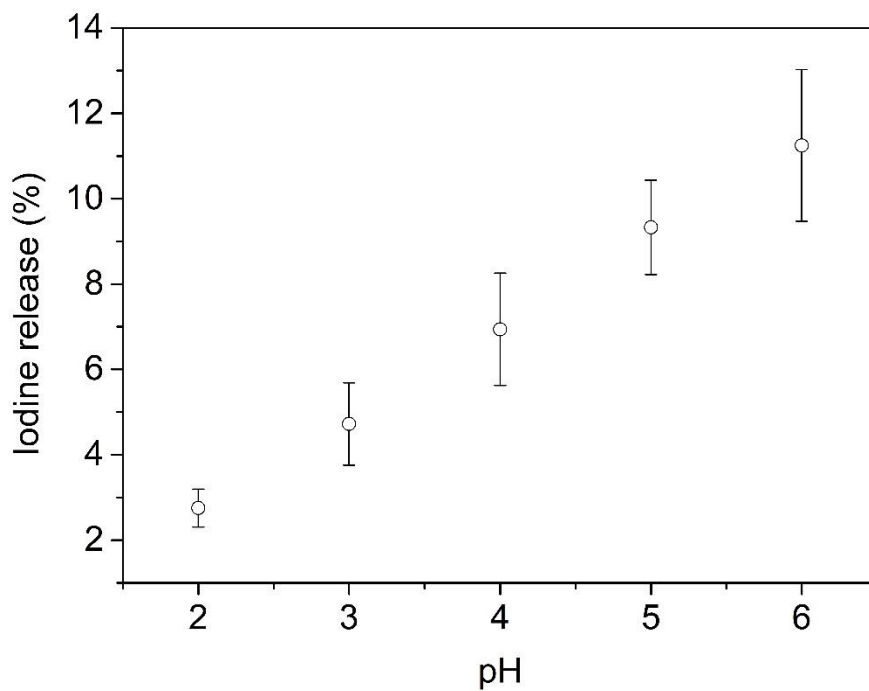


Fig. S8. Quantification of the released I_2 formed from IO_3^- (product of I_2O_5 hydrolysis) reduction by 1-phenylethanol in the particle phase, as a function of pH value. The pH of the aqueous solution was adjusted with 2 M H_2SO_4 or 2 M NaOH. Errors (2σ) ranged between 5.8% and 19.7% and were determined from triplicate runs of three individual samples for each data.

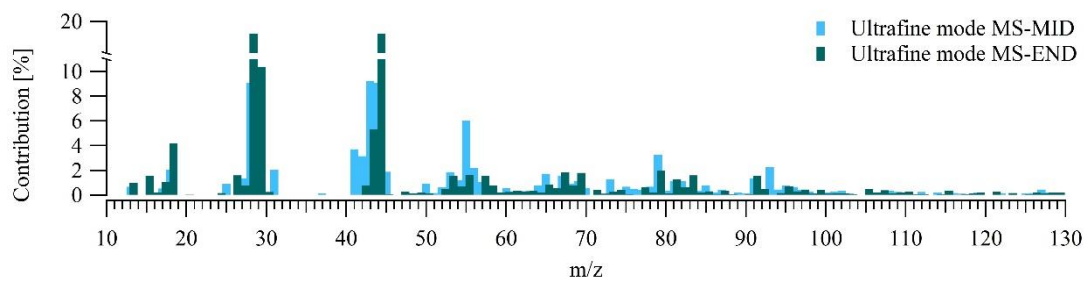


Fig. S9. Mass spectra of different ultrafine aerosol mode growth stages: MID (light blue) is mid-growth of the ultrafine event and END (dark blue) is the final stage of the event as presented in Fig. 1 of the main text.

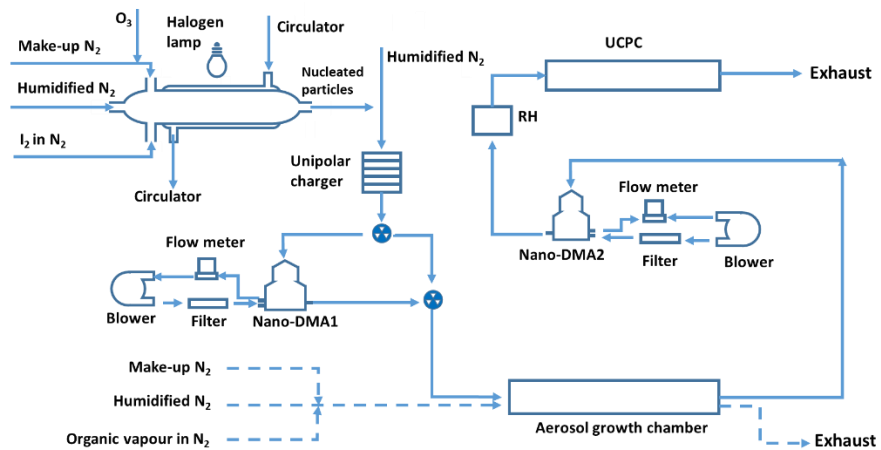


Fig. S10. Schematic of experimental set-up for particle growth measurement.